Experimental and Numerical Investigation of Mould Growth Risk on Wooden Load-Bearing Structure in Hemp-lime Concrete Facades

S Petersen[1], S Svendsen[2] and M Hahn-Hundsdahl[3]

[1]Department of Civil and Architectural Engineering, Aarhus University, Aarhus, Denmark
[2]LB Consult, Klostergade 30, 8000 Aarhus, Denmark
[3]Rambøll A/S, Olof Palmes Allé 20, 8200 Aarhus, Denmark

Abstract. The need for reducing the environmental impact of the production of building materials has accelerated the emergence of new types of bio-based façade systems. Some of these systems are claimed to have hygro-thermal properties that eliminate the need for a dedicated air and/or vapour barrier as a part of the façade buildup. This paper presents a risk assessment of moisture-related deterioration of the wooden load-bearing structure in an existing hemp-lime concrete building façade system constructed without a dedicated air or vapour barrier in Aarhus, Denmark. Destructive investigation found no mould on structure. The façade was then modelled in WUFI 2D and calibrated using time series data from field measurements of temperature and relative humidity internally in the construction and in its surroundings. The calibrated WUFI model was used to simulate the annual moisture cycle using different initial conditions and weather data. The simulation output was analysed for the risk of mould growth at the wooden load-bearing structure using the Mould Growth Index. Results indicate that the initial moisture content of materials, the position of the wood structure, and the season of construction completion is important to consider to minimise risk of mould growth in the build-up.

1. Introduction

The need for reducing the environmental impact from the production of building materials has accelerated the emergence of bio-based thermal insulation materials. These materials are intended to substitute conventional materials in the opaque parts of the building enclosures to bring down the environmental impact of buildings in a life-cycle perspective. However, a modern opaque façade has several functions other than thermal insulation. One of them is that the build-up of the façade must also minimise the risk of moisture-related damages. Some proposed façade systems making use of bio-based materials for thermal insulation are claimed to have hygro-thermal properties that eliminate the need for a dedicated air and/or vapour barrier as a part of the façade build-up. One of them is the in situ casted hemp-lime concrete façade with embedded wooden load-bearing structure intended for new buildings in temperate coastal climates featured in this paper, see Figure 1.

The current body of literature seems to contain very few studies that features the hygrothermal performance of facades containing the hemp-lime material. Dhakal et al. [1] made a numerical simulation of two wall assemblies with either lime render or a wooden cladding with ventilated air gap in front of 300 mm hempcrete and 15 mm lime plaster located in Ontario, Canada. They concluded that this diffusion-open build-up perform well in all the hygrothermal parameters without any deleterious issues. No mould growth predictions were conducted. The façade build-up has no embedded wooden load-bearing structure as the build-up featured in this paper.

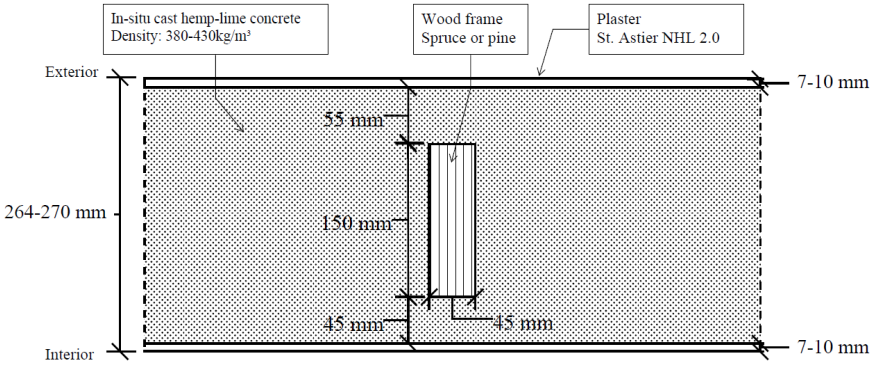


Figure 1. Build-up of the façade featured in this study.

Latif et al. [2] conducted environmental chamber tests of a build-up with a combination of a layer of woodfiber and a layer of hemp-lime for thermal insulation. No wooden load-bearing structure was involved. This build-up had a relative humidity between the two layers close to 80% during a design winter dynamic profile – level that which is critical for mould growth on e.g. wood. No investigations of build-ups that combine hemp-lime with an embedded wooden load-bearing structure was identified. However, it is known from reports on investigations of insulated wood-frame walls using bio-based thermal insulation materials, e.g. Pihelo et al. [3], Latif et al. [4], Latif et al. [5], that it is not without risk of moisture-related problem to construct such facades without a dedicated vapour barrier in temperate and cold climates. There are thus good reasons for conducting a hygrothermal investigation of the mould growth risk of the build-up as per Figure 1.

2. Method

The study applied data collected from field measurement of a full-scale house to calibrate a numerical model for long-term evaluation of mould risk assuming different initial conditions and weather data. It is noted that a destructive investigation found no mould on existing structure. The following sections provides details about the data collection.

2.1. Field measurements

A measurement campaign at an allotment house with facades constructed as depicted in Figure 1 was conducted for a period of approx. 137 days (01/06-2021 at 12.00 to 11/10-2021 at 14.00) approx. nine months after it was constructed. The house was constructed in 2020 and is located in the western suburbs of Aarhus, Denmark (approx. 56.2°N, 10.1°E). Figure 2 depicts the house together with its floor plan.

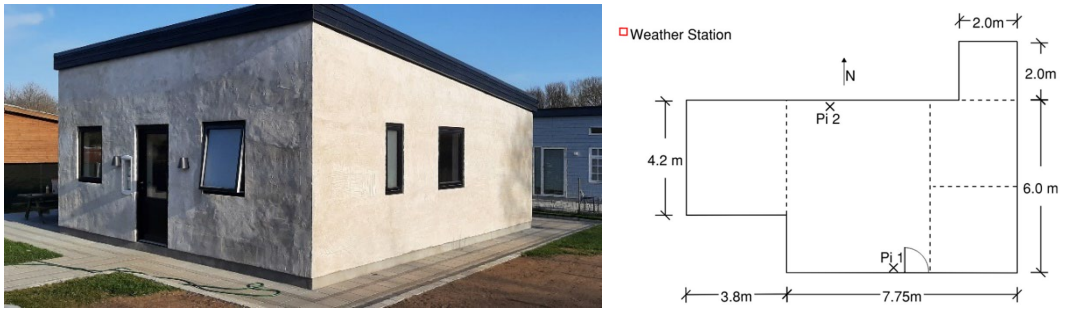


Figure 2. The allotment house (left) and its floor plan (right). The floor plan indicate dimensions of the house as well as position of the equipment for measurements.

The temperature and relative humidity across the façade was measured at two locations, *Pi 1* and *Pi 2* indicated in Figure 2 (right). Two Raspberry Pi-based temperature and humidity loggers were constructed for this purpose. Each Pi collected and stored data from five Adafruit Sensirion SHTC3 Temperature & Humidity Sensors (STEMMA QT/Qwiic) with a measurement precision of ±0.2˚C and

±3% relative humidity at T=25 ˚C. No calibration was conducted as all sensors were brand new and calibrated by manufacturer before shipment. Measurement were logged every 20 minutes. Figure 3 indicate the position of the sensors on the surface and inside the wall at the two locations. A diamond core drill was used to bore out three cores of different depths alongside a wooden load-bearing stud inside the wall. A sensor was placed in each borehole before they were closed again with the bore core. A sensor was also placed on the internal and external surface, respectively. The outdoor sensor was shielded from sun and rain.

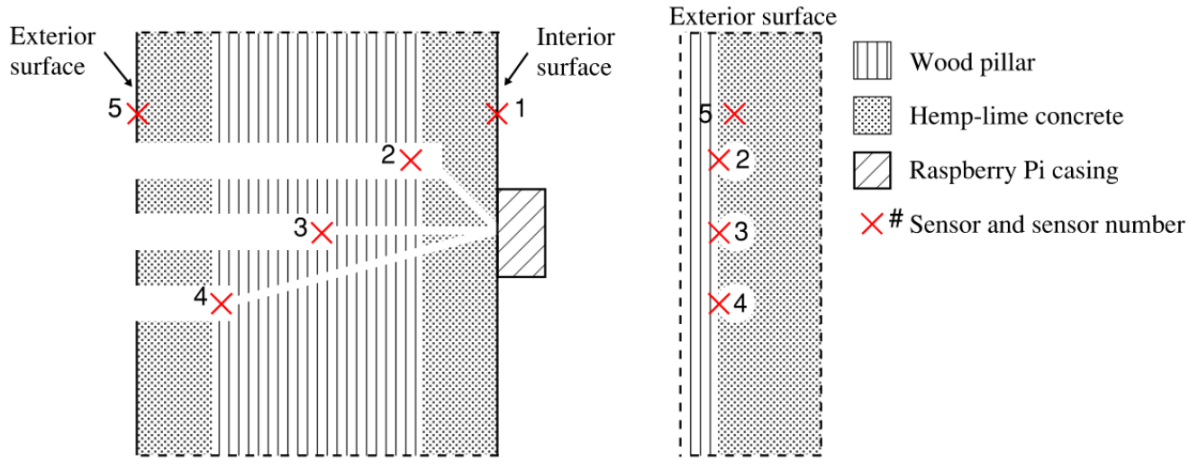


Figure 3. The position of the sensors on the surface and inside the wall at the two locations *Pi1* and *Pi2* in Figure 2.

A mobile weather station Delta T Devices WS GP1 was installed nearby the building as indicated in Figure 2 at a height of 4m which was slightly above roof height. The weather station logged air temperature (±0.3˚C), relative humidity (±0.3% at T=23˚C), wind speed (±0.1 m/s), wind direction (±4˚), global horizontal solar radiation in W/m^2 (±5%), and Precipitation in mm (-). Measurements were logged as 20-minute average values.

2.2. Numerical model

A numerical model of the façade shown in Figure 1 was created in *WUFI 2D* [6]. The specific material properties of the materials used in the allotment house are unknown. A literature review to identify the material properties needed for the various storage and transport functions of WUFI 2D was therefore conducted. Table 1 list the identified properties used in the initial WUFI 2D model. Wood material properties are set to be the same as for *Spruce, tangential* from the *WUFI* material library. The properties of lime plaster was from Banfill [7] while the properties of hemp-lime concrete was collected from various sources. The hemp-lime concrete layer was divided into three sub-layers of equal thickness as data from the field measurements indicated a need to differentiate the initial moisture conditions throughout the layer; the relative humidity was set to 87%, 82%, and 68% for the outer, middle, and inner layer, respectively. WUFI weather data files to represent external boundary conditions were generated using data from the field measurements. Solar radiation, wind direction and speed, and precipitation was from the weather station data while air temperature and relative humidity was from the outdoor measurements conduced at the location of Pi2 (Figure 2). Internal boundary conditions were air temperature and relative humidity measured indoors at the same location. The timestep was set to 60 minutes, and a medium size mech was found to have an acceptable trade-off between convergence and computational time. A calibration procedure was conducted where the material properties for the hemp-lime concrete in the initial WUFI model (Table 1) was adjusted so that the output from WUFI fitted the measurements from the field experiment.

Table 1. Material properties in the initial WUFI model.

	Plaster	Hemp-lime concrete
Bulk density ρ $[kg/m^3]$	1937	400
Thermal conductivity λ $[W/(m \cdot K)]$	0.62	0.15*
Moisture-dependent thermal conductivity $[\%/(M\%)]$	6	0.4
Specific heat capacity c_p $[J/(kg \cdot K)]$	814	1500
Vapour permeability δ_p $[kg/(m \cdot s \cdot Pa)] \cdot 10^{-12}$	11.9	5
Porosity [%]	21.8	70
Typical Built-in moisture $[kg/m^3]$	184	280
Reference water content $[kg/m^3]$	11.6	30
Water absorption coefficient $[kg/(m^2 \cdot \sqrt{s})]$	12.3	0.073
Maximum water content $[kg/m^3]$	-	700

*λ-value estimated to be 1.5 times higher than the typical dry-state λ-value of 0.1.

The calibration procedure started with a sensitivity analysis using the *differential sensitivity analysis* technique of the material properties (Table 2). The purpose of the sensitivity analysis was to identify which input variables that has the greatest influence on the variation of the output; these inputs (Table 3 and 4) were included in the calibration of the initial WUFI model.

Table 2. Hemp-lime concrete material properties subject to sensitivity analysis.

	Initial	Upper	Lower
Bulk density ρ $[kg/m^3]$	400	700	100
Thermal conductivity λ $[W/(m \cdot K)]$	0.1	0.16	0.04
Moisture-dependent thermal conductivity $[\%/(M\%)]$	0.4	0.7	0.1
Specific heat capacity c_p $[J/(kg \cdot K)]$	1500	2000	1000
Water vapour diffusion resistance factor [-]	4	11.6	2.5
Liquid Transport Coefficient, Suction	Function from [8]	Multiply by 1000	Divide by 1000
Liquid Transport Coefficient, Redistribution	Function from [8]	Multiply by 1000	Divide by 1000
Moisture Storage Function	Function from [9,10]	Multiply by 2	Divide by 2
Interior Surface Heat Transfer Coefficient $[W/(m^2K)]$	8	13	3
Exterior Surface Heat Transfer Coefficient $[W/(m^2K)]$	17	22	12
Initial relative humidity [%] (Outer, middle, and inner layer)	87, 82, and 68	+ 10 %-points	- 10 %-points
Short-wave absorptivity [-]	0.4	0.8	0.2

The next step in the calibration procedure was to split the data from the location of Pi2 (north façade) of the field experiment into a *Training Dataset* and a *Validation Dataset*. The *Training Dataset* was used in the calibration procedure to identify the best combination of inputs using Goodness-of-fit (GoF)

as statistical index to evaluate model prediction. The calibrated model was simulated using weather data from the Validation Dataset and subsequently compared to the temperature and relative humidity measurements across the façade using GoF. However, trial runs prior to actual calibration revealed that calibration with respect to relative humidity produce unreliable results. Calibration using water content would produce more reliable results, and calibration was therefore conducted with respect to the moisture content expressed by a mixing ratio of a parcel of moist air inside the construction assuming that the parcel is in equilibrium with the material in the construction.
The model was first calibrated with respect to the temperature measurements from the field experiment by adjusting the thermal input variables within the intervals listed in Table 3 assuming no influence from moisture conditions (moisture calculations disabled in WUFI). All combinations within these intervals were explored leading to 1500 simulations.

Table 3. Hemp-lime concrete thermal material properties included in calibration.

	Low	Highest	Step size	Number of steps
Bulk density $[kg/m^3]$	300	500	50	5
Thermal conductivity $[W/(m \cdot K)]$	0.13	0.4	0.03	10
Heat capacity $[J/(kg \cdot °C)]$	1000	2000	250	5
Short-wave absorptivity $[-]$	0	0.16	0.02	6

The moisture calculations were then reactivated, and the calibration procedure was repeated for the moisture-related input variables (Table 4). All combinations led to a total of 972 simulations. Manual adjustments of various inputs to the model with the best fit was then conducted to investigate whether it was possible to obtain an even better fit.

Table 4. Hemp-lime concrete hygric material properties included in calibration.

	Plaster			Hemp-lime concrete		
	Value 1	Value 2	Value 3	Value 1	Value 2	Value 3
Water vapour resistance factor	14	100	200	0.5	1	3
Liquid Transport, Suction	WUFI Function	Multiply by 1000	Multiply by 0.001	Function from [8]	Multiply by 1000	-
Liquid Transport, Redistribution	WUFI Function	Multiply by 1000	Multiply by 0.001	Function from [8]	Multiply by 1000	-
Moisture Storage Function						
75% RH				28	35	42
80% RH				33	35	37
90% RH				34.75	35	35.25

The final calibrated model was then subject to a long-term assessment of mould growth risk. For this purpose, an hourly simulation using the Danish design reference year [11] repeated for a five-year period as external boundary conditions, and the internal conditions were constructed from the indoor field measurement data. Data from the field measurements is used as initial material temperatures and moisture conditions. The mould growth risk was assessed using the *Mould Growth Index, M,* calculated by *WUFI*-plugin, *WUFI Mould Growth Index VTT*. The index *M* was calculated at the same point as sensor point 4 in Figure 3, i.e. at a point on wood pillar closest to the exterior, which is assumed to be where the risk of mould growth is largest in general. The index *M* was calculated for the different levels

of initial moisture content in the different layers: A *Low* scenario where the initial relative humidity is 60% in the Hemp-lime concrete and wood, and 90% in the plaster (assumed to be the conditions if the façade was constructed from dry hemp-lime concrete, e.g. prefabricated blocks), a *Medium* scenario that corresponds to the conditions measured in the field experiment, and a *High* scenario where the initial relative humidity is 95% in the Hemp-lime concrete, 80% in wood, and 90% in the plaster (wet in-situ cast hemp-lime concrete). Furthermore, calculations were conducted for three WUFI Mould Growth Index VTT sensitivity classes: Very Sensitive (Untreated wood, includes lots of nutrients for biological growth), Sensitive (Planned wood, paper coated products, wood-based boards), and Medium Resistant (Cement or plastic-based materials, mineral fibres). It is noted that the wood in the façade build-up is most likely planned wood and therefore in the class *Sensitive* but it could also be in *Medium Resistant* due to potential protecting effect of alkaline limestone in hemp-lime concrete [12]. The position of the wooden studs in the façade build-up was also investigated moving the stud 45 mm towards the interior surface to obtain a general increase of the temperature at the outer surface of the stud. The final investigation was on the façade completion season – either spring (May) or fall (September).

3. Results and Discussion

Figure 4 depicts the measured temperature and relative humidity as well as the derived mixing ratio together with the output from the calibrated WUFI model for two locations inside the façade build-up, namely sensor point 4 (close to outer surface) and sensor point 3 (middle of construction) illustrated in Figure 4 left and right, respectively. The GoF for temperature and mixing ratio was approx. 81% and 77% at both sensor points. Despite of similarity in GoF, it seems visually that the fit for sensor point 4 is slightly more accurate than for sensor point 3. Furthermore, relative humidity is higher at sensor point 4 than sensor point 3 which indicate that this could also be the appropriate location to evaluate risk of mould growth. Overall, it seems like the calibrated model is appropriate for the subsequent mould growth analysis.

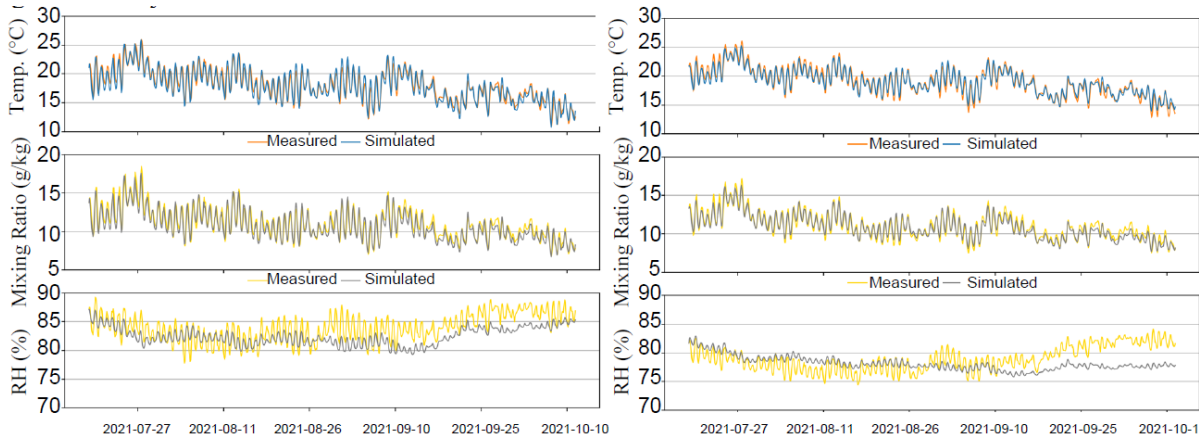


Figure 4. Measured and simulated temperature and relative humidity, and the derived mixing ratio for sensor point 4 (left) and sensor point 3 (right) as per Figure 3.

Figure 5 depicts the hourly temperature, relative humidity, and Mould Growth Index at sensor point 4 for the five consecutive years of simulation. Simulations after this point in time is expected to basically repeat the pattern of the fifth year. The relative humidity is decreasing over the first three years and stabilises at the fourth year. There is a high relative humidity during winter, and less in the summer. Mould may occur during first years ($M > 1$) but the risk diminishes over the years as the façade dries. Figure 6 shows the Mould Growth Index at sensor point 4 for the five consecutive years of simulation with different initial moisture content. The *High Moisture Content* has $M > 4$ over a period of almost four years which is very critical. The *Medium Moisture Content* is somewhat critical in year 1 and year 2 ($M > 2$). *Low Moisture Content* has an increasing Mould Growth Index over time but it never becomes $M > 1$. The index for *Low Moisture Content* and *Medium Moisture Content*

reaches the same level in Year 5. Figure 7 indicate critical conditions if wood components are categorised as *Very Sensitive*. Despite significant declines in Mould Growth Index during drying periods, increase in wetting periods is almost as high causing favourable conditions for mould growth in all five years. If categorized as *Medium Resistant* the index becomes close to zero. This is the likely category for the investigated build-up as *Medium Resistant* provided that wooden structure was coated in lime-binder during the in situ casting. Mould growth is strongly limited in alkaline environments at pH-level above 9.5 [12,13] and non-carbonated hemp-lime concrete has a pH-level at 10-12 [12,14]. However, carbonation decreases the alkalinity during the curing process; depending on mixing formula, lime-binder type and its initial pH-level, pH-level may become below 9.5 [15] when fully carbonated. Figure 8 shows the Mould Growth Risk at sensor point 4 (Figure 3) depending on its distance from the exterior surface of the façade and indicates that moving wood materials toward warm interior side of the façade reduces the index to zero after less than a year. Figure 9 shows the Mould Growth Risk at sensor point 4 (Figure 3) depending on the completion season and indicates that completion in spring (May) results in lower Mould Growth Index than fall (September).

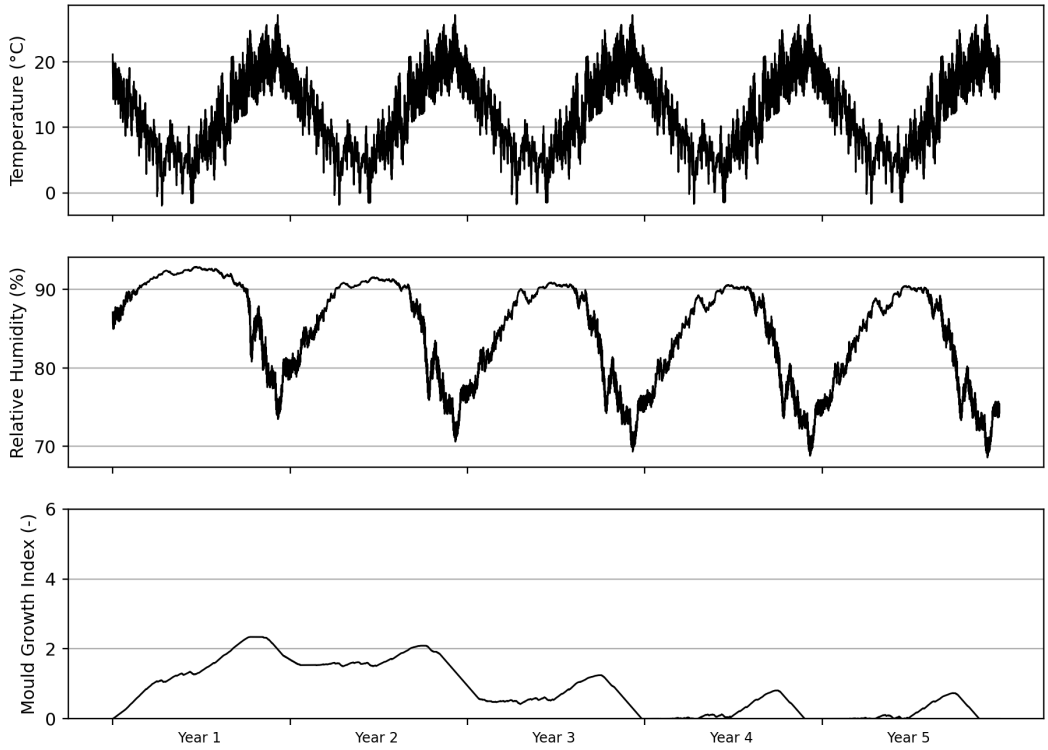


Figure 5. Simulated temperature and relative humidity, and the derived mixing ratio for sensor point 4 in Figure 3.

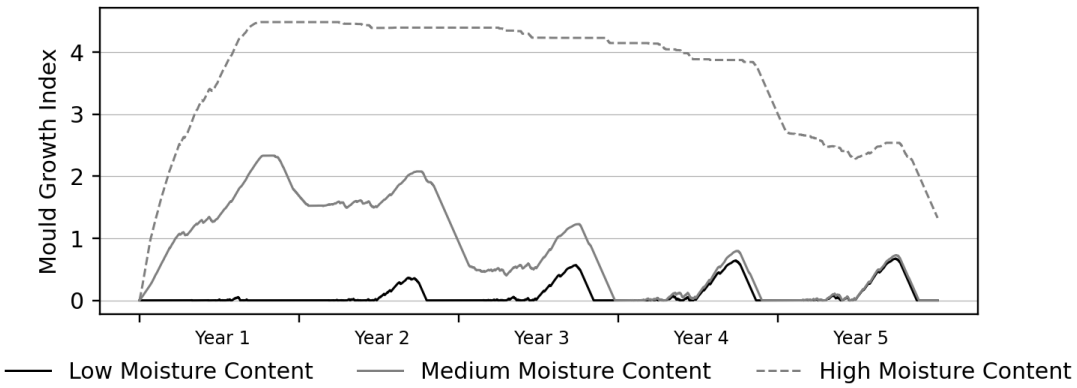


Figure 6. Mould Growth Index at sensor point 4 with different initial moisture content.

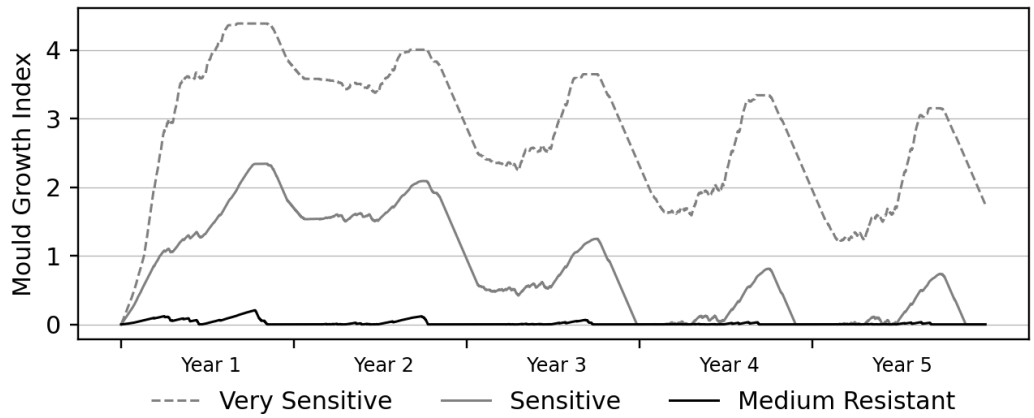


Figure 7. Mould Growth Index at sensor point 4 for different sensitivity categories.

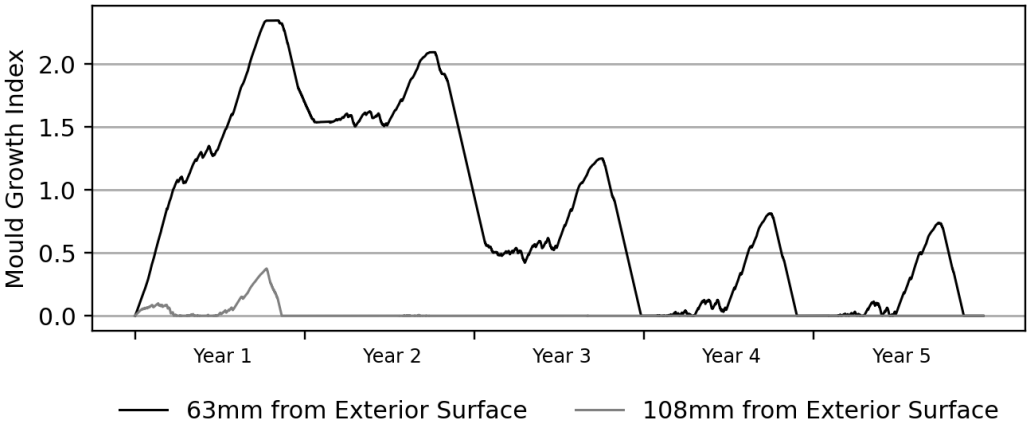


Figure 8. Mould Growth Index at sensor point 4 for initial model (63 mm) and when the stud is moved 45 mm inward.

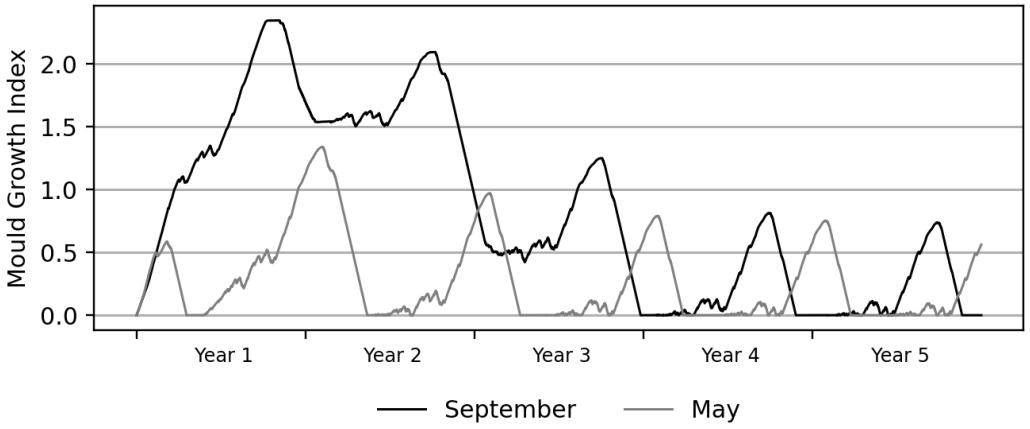


Figure 9. Mould Growth Index at sensor point 4 for two different completions.

4. Conclusion

The investigation of an in-situ hemp-lime concrete façade build-up without a dedicated air and moisture barrier indicate that the build-up starts out having a moderate Mould Growth Risk but that it likely drops to a low risk as the façade dries out over a few annual cycles. A parametric analysis

indicate that the Mould Growth Risk is highly affected by the initial moisture content in the build-up, the position of the load-bearing structure in the build-up, and the construction completion season. To minimize the Mould Growth Risk in the investigated build-up in the Danish climate, it is therefore recommended that the hemp-lime concrete does not have a high initial water content, that the wooden bearing structure should be moved as far towards the warm interior side of the façade as possible, and that the construction should be the completed during spring (May) rather than fall (September).

5. References

[1] Dhakal, U., et al., Hygrothermal performance of hempcrete for Ontario (Canada) buildings. Journal of cleaner production, 2017. 142: p. 3655-3664.

[2] Latif, E., et al., An experimental investigation into the comparative hygrothermal performance of wall panels incorporating wood fibre, mineral wool and hemp-lime. Energy and Build, 2018. 165: p. 76-91.

[3] Pihelo, P., et al., Field Study on Hygrothermal Performance of Highly Insulated Exterior Wall in Estonia. 12th REHVA World Congr. CLIMA, 2016: p. 22-25.

[4] Latif, E., et al., Hygrothermal performance of wood-hemp insulation in timber frame wall panels with and without a vapour barrier. Building and Environment, 2015. 92: p. 122-134.

[5] Latif, E., M.A. Ciupala, and D.C. Wijeyesekera, The comparative in situ hygrothermal performance of Hemp and Stone Wool insulations in vapour open timber frame wall panels. Construction and Building Materials, 2014. 73: p. 205-213.

[6] Wufi. WUFI 2D. Fraunhofer Institute for Building Physics. 2022.

[7] Banfill, P.F.G. Hygrothermal properties of NHL mortars. In: 3rd International Conference on Energy Efficiency in Historic Buildings (EEHB2018), Visby, Sweden, 2018. Uppsala University.

[8] Evrard, A. and A. De Herde, Hygrothermal performance of lime-hemp wall assemblies. Journal of building physics, 2010. 34(1): p. 5-25.

[9] Le, A.D.T., et al., Effect of Temperature Dependence of Sorption on Hygrothermal Performance of a Hemp Concrete Building Envelope. Encyclopedia of Renewable and Sustainable Materials, Elsevier, 2020. 2: p. 68-77.

[10] Collet, F., et al., Comparison of the hygric behaviour of three hemp concretes. Energy and Buildings, 2013. 62: p. 294-303.

[11] Wang P.G., et al., 2001 – 2010 Danish Design Reference Year, in Technical Report 13-19. Danish Meteorological Institute.

[12] Viel, M., et al., Resistance to mold development assessment of bio-based building materials. Composites Part B: Engineering, 2019. 158: p. 406-418.

[13] Andersen, B., et al., Kontrol og forebyggelse af skimmelsvampevækst ved indvendig efterisolering: Laboratoriebaserede undersøgelser af materialers vandaktivitet og pH i forhold til skimmelsvampevækst. 2020.

[14] Benmahiddine, F., et al., Experimental investigation on the influence of immersion/drying cycles on the hygrothermal and mechanical properties of hemp concrete. Journal of Building Engineering, 2020. 32: p. 101758.

[15] Marceau, S., et al., Influence of accelerated aging on the properties of hemp concretes. Construction and Building Materials, 2017. 139: p. 524-530.